Earth, Moon, and Planets (2005) 97: 435–458
DOI 10.1007/s11038-006-9069-7

The Dynamics of Objects in the Inner Edgeworth–Kuiper Belt

DANIEL C. JONES and IWAN P. WILLIAMS
Astronomy Unit, Queen Mary, University of London, Mile End Road, London, E1 4NS, UK
* E-mail: d.c.jones@qmul.ac.uk

MARIO D. MELITA
IAFE, Universidad De Buenos Aires, Ciudad Universitaria, Buenos Aires, República Argentina

(Received 10 November 2005; Accepted 10 March 2006)

Abstract. Objects in 3:2 mean motion resonance with Neptune are protected from close encounters with Neptune by the resonance. Bodies in orbits with semi-major axis between 39.5 and about 42 AU are not protected by the resonance; indeed due to overlapping secular resonances, the eccentricities of orbits in this region are driven up so that a close encounter with Neptune becomes inevitable. It is thus expected that such orbits are unstable. The list of known Trans-Neptunian objects shows a deficiency in the number of objects in this gap compared to the 43–50 AU region, but the gap is not empty. We numerically integrate models for the initial population in the gap, and also all known objects over the age of the Solar System to determine what fraction can survive. We find that this fraction is significantly less than the ratio of the population in the gap to that in the main belt, suggesting that some mechanism must exist to introduce new members into the gap. By looking at the evolution of the test body orbits, we also determine the manner in which they are lost. Though all have close encounters with Neptune, in most cases this does not lead to ejection from the Solar System, but rather to a reduced perihelion distance causing close encounters with some or all of the other giant planets before being eventually lost from the system, with Saturn appearing to be the cause of the ejection of most of the objects.

Keywords: Celestial mechanics, Numerical methods: N-body, Trans-Neptunian objects

1. Introduction

Both Edgeworth (1943) and Kuiper (1951) independently stated that there was no obvious reason the material out of which the planets formed should suddenly stop at the distance of Pluto, and consequently postulated that a belt of smaller bodies should exist beyond Pluto (it should be remembered that at the time it was accepted that Pluto was slightly larger than the Earth in size so that many regarded it as the natural end to the Solar System). Edgeworth also argued that comets could originate from this belt. In this picture, the bodies had formed out of the Solar Nebula and so were assumed to be moving in near circular orbits close to the ecliptic. Most astronomers ignored these ideas until the late 1980s, when computer simulations (e.g. Duncan et al., 1988; Stagg and Bailey, 1989; Quinn et al., 1990) showed that the short period comets could not be produced from the Oort Cloud in

sufficient numbers to match the observations. Hence the need arose for the existence of a belt of co-planar objects beyond the known planets but inside the Oort Cloud; in other words, the Edgeworth–Kuiper Belt. This need prompted observers to search for the belt.

One of the early searches was by Kowal (1989). This was unsuccessful in finding objects beyond Pluto, but did discover the first member of a new class of objects, now called *Centaurs*, namely 2060 Chiron. This class of objects orbit in the Saturn–Uranus–Neptune region of the Solar System and so the orbits are likely to be unstable over the age of the system. This implies that they have been inserted into their present orbits in the fairly recent past. Thus, though Kowal failed to discover any objects belonging to the Edgeworth–Kuiper Belt, he may well have discovered an object that was once a member. The first Edgeworth–Kuiper Belt body to be discovered was 1992 QB1 (now officially 15760 but still better known by its temporary designation) by Jewitt and Luu (1993). 1992 QB1 has an orbit with a semi-major axis of 43.734 AU, an eccentricity of 0.065 and an inclination of 1.9°. It is thus exactly what was expected of an object belonging to the Edgeworth–Kuiper Belt: a low inclination, near circular orbit a little beyond Pluto. It was not long before the picture became more complicated. Object 15789 (temporary designation 1993 SC) was shown by Williams et al. (1995) to be moving in an orbit that is in 3:2 mean motion resonance with Neptune. The semi-major axis of its orbit is 39.161 AU and its eccentricity is 0.318, very similar to that of Pluto. This was to be the first of a fairly populous class of objects, now popularly called the *Plutinos*, that move in mean motion resonance with Neptune. The origin of these bodies and their capture into resonance are both very interesting topics, but are not of prime concern to this work, other than the fact that their location forms a convenient inner boundary to the region of interest to us.

Since then, many other bodies have been discovered that do not move in orbits that are consistent with the classical Edgeworth–Kuiper picture; they have large semi-major axes and high eccentricities (Luu et al., 1997). They are popularly called the *scattered disk objects* since the initial suggestion for their formation was that they had been scattered into such orbits by close encounters with Neptune (Duncan and Levison, 1997; Maran and Williams, 2000). However some of the scattered disk members have perihelion distances so large that major perturbations from Neptune are unlikely (Gladman et al., 2001) and other theories for their origin have been proposed (Collander-Brown et al., 2001; Fernandez et al., 2003; Gomes, 2003; Levison and Morbidelli, 2003). In order to explain the significant number of bodies trapped in the 3:2 resonance, Malhotra (1995) suggested that outward radial migration of Neptune could enhance the number of such objects captured. In addition, Levison and Morbidelli (2003) suggested that many of the features of the belt could be explained if the whole belt initially

formed closer to the Sun and was pushed outwards as a consequence of the early outward migration of Neptune. More recently, Tsiganis et al. (2005) have suggested that many of the features of the present Solar System can be explained through the outward migration of the planets. In this work, we do not consider planetary migration but investigate the evolution of part of the belt within the Solar System as it is today. The region that will be discussed is in the inner region of the Edgeworth–Kuiper Belt: the region from about 40 AU (the outer edge of the 3:2 resonance) to 43 AU. As we will see, the population density in this region is very low compared to that in the remainder of the belt and is also low compared to what might be expected from the generally accepted accretion disk model for the formation of the Solar System. In this work we describe the results of numerical simulations of the evolution of this part of the belt under the effect of gravitational perturbations from the known planets. As a by-product of our main investigation, a possible explanation for the orbits of some of the scattered disk objects will emerge.

2. The Present Situation in the Inner Edgeworth–Kuiper Belt

Figure 1 is a plot of eccentricity, e, against semi-major axis, a, for all the known Edgeworth–Kuiper objects. The main dynamical features of the region can be clearly seen. For example, the Plutinos are clearly visible as a vertical band situated just inside 40 AU. The scattered disk is composed of those objects with eccentricity greater than about 0.2 and semi-major axis extending

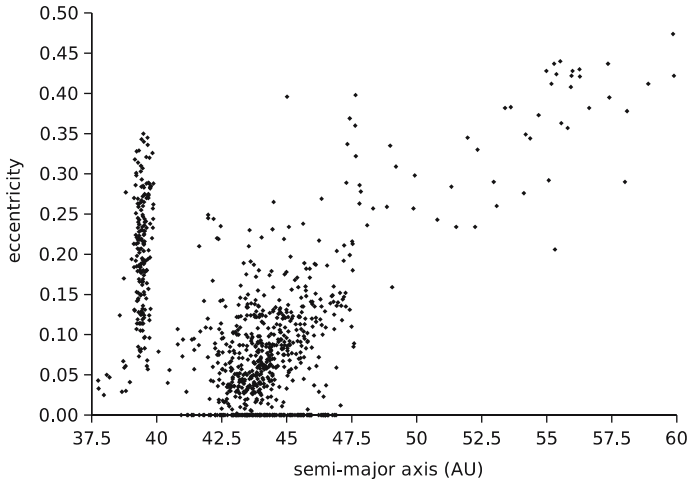

Figure 1. A plot of eccentricity against semi-major axis for observed Edgeworth–Kuiper Belt objects between 37.5 and 60 AU.

to values of nearly 80 AU. We also see a sharp edge to the classical belt at around $a = 48$ AU. The region of interest to us is the gap that appears to be present with $40 \leq a < 43$ AU. Figure 2 is a histogram which shows the number of known objects in the Edgeworth–Kuiper Belt on 5th October 2005 in bins of width 1 AU near the region of interest to us, namely $38 \leq a < 48$ AU. Again, it is obvious from this figure that there is a large number of objects captured in 3:2 mean motion resonance with Neptune, which is situated at $a = 39.4$ AU. The reason that these objects have survived in orbits that pass very close to the orbit of Neptune is that the resonance prevents actual close encounters with the planet. However, close to the resonance zone, but not in it, exactly the opposite may be true. Objects will inevitably experience close encounters with Neptune. Further, since the eccentricities of such orbits can be driven up and the perihelion distance reduced by Neptunian perturbations, orbits that were initially some distance from the orbit of Neptune can evolve until they cross Neptune's orbit, resulting in an inevitable close encounter.

As can be seen from Figure 1, the number of objects with $a < 50$ AU and $e > 0.25$ is very small, not counting the 3:2 resonance. Since perihelion distance, q, is given by

$$q = a(1 - e),$$

a simple calculation shows that for an object with $a > 43$ AU and $e < 0.25$, $q > 32.25$ AU. Hence, objects in orbits with $a > 43$ AU within the classical Edgeworth–Kuiper Belt cannot have close encounters with any major object and can be expected to be in very stable orbits. Numerical integrations by Duncan et al. (1995) and Malhotra et al. (2000) have clearly demonstrated

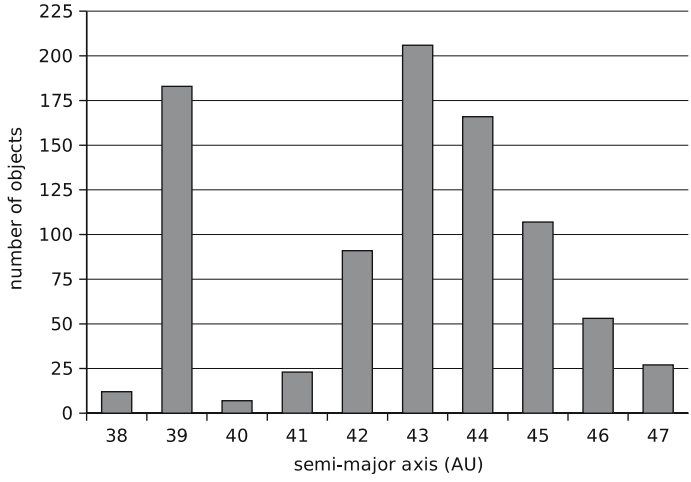

Figure 2. A histogram showing the number of observed Edgeworth–Kuiper Belt objects in each 1 AU interval in semi-major axis between 38 and 48 AU.

that this is the case. The 2:1 mean motion resonance with Neptune is situated at approximately $a = 47.5$ AU. However, in contrast to the situation close to the 3:2 mean motion resonance, we do not see any enhancement in the population at this location. This mirrors the situation in the asteroid belt, where the 2:1 resonance (with Jupiter) appears devoid of asteroids compared to the surrounding population, while the 3:2 resonance region shows an enhancement (see for example Binzel, 1989). Again, however, one might expect some disturbance to the orbits close to semi-major axis values associated with the resonance, leading to a reduction in the population density. In Figure 2, we do clearly see such a decrease as the resonance is approached. What is not expected is that the population does not recover at distances beyond 47.5 AU. Indeed, one of the major dynamical problems currently under debate, which we do not enter into here, is to find an explanation for the decline to near zero in the population of the classical Edgeworth–Kuiper Belt beyond 47.5 AU (e.g. Melita et al., 2004; Melita et al., 2005), that can be clearly seen in Figure 1.

From Figure 2, it is clear that the number of objects reaches a maximum in the region where $43 \leq a < 45$ AU. From $a = 45$ AU to $a = 47.5$ AU there is a steady decline in numbers towards the location of the 2:1 resonance. In passing, it worth noting that there is a slight distortion in the histogram box 47–48 AU: there are no objects beyond 47.5 AU, hence the number in this box is in reality the number in a 0.5 AU gap, and to be compared with other boxes, the number should be doubled. The number of objects with $43 \leq a$ AU is 370, or 185 per 1 AU box on average. If we extend the region to $43 \leq a < 46$ AU, the average number of objects per box drops to 160. In the gap between 40 and 41 AU there are seven objects which represents about 3.8% of that observed in the most densely populated part, the 43–45 AU region, or 4.4% of the population between 43 and 46 AU. The population between 41 and 42 AU numbers 23 objects, or about 12.4% of the population of the densest region, while the population between 42 and 43 AU is 91 objects or about 49% that of the densest region.

However, observational biases lead to a greater number of fainter objects being observed at smaller heliocentric distances. This is simply due to the greater apparent magnitudes of these objects. To take account of this we must estimate of the number of objects at larger heliocentric distances which are not observable and make adjustments to our population estimates. To find the relative sizes of two objects situated at heliocentric distances, with equal apparent magnitude, m, we use the standard apparent magnitude formula

$$m = m_{\odot} - 5\log(R) + 2.5\log\left(\frac{\Delta^2 r^2}{Ap(\chi)}\right),$$

where $m_\odot$ is the apparent magnitude of the Sun, R is the radius of the observed object and A is its albedo, Δ is the object's geocentric distance and r is its heliocentric distance. Using the Sun–Earth-Object geometry at opposition we have $\Delta = r - 1$ AU and the phase integral, $p(\chi)$ is the same for all objects. Setting the apparent magnitudes of two bodies with radii, R_1 and R_2 at heliocentric distances r_1 and r_2 respectively to be equal, and assuming both objects have equal albedoes and are at opposition, we have

$$\frac{R_1}{R_2} = \frac{r_1(r_1 - 1\,\mathrm{AU})}{r_2(r_2 - 1\,\mathrm{AU})}.$$

This gives the ratio of the sizes of two bodies at r_1 and r_2 with equal apparent magnitudes. Now taking the centre of the region under inverstigation relative to the centre of the 43–45 AU region, i.e. $r_1 = 44$ AU and $r_2 = 41.5$ AU, we have, $R_1/R_2 = 1.126$. We can use a size distribution of $n(R > R_{\min}) = \Gamma R_{\min}{}^{-q}$, with $q = 4$ and Γ is a normalising constant, as in for example Trujillo et al. (2001), to get the ratio of

$$\frac{n(R_2)}{n(R_1)} = \left(\frac{R_1}{R_2}\right)^4 = 1.606,$$

where $n(R_1)$ and $n(R_2)$ are the number of objects with radius above R_1 and R_2 respectively. So to take account of biases in the observed populations due to apparent magnitude differences we need to multiply the 44 AU population by 1.606.

Because most surveys are restricted to a small band around the ecliptic, there is also an observational bias in favour of the classical belt because of their lower inclinations. Given that γ is the angle away from the ecliptic plane which defines the band in which surveys are conducted, the probability of detecting an object at a given inclination, I is

$$P(I) = (2/\pi)\arcsin(\sin\gamma/\sin I),$$

where $\gamma < I < \pi/2$ and Collander-Brown et al. (2003) give $\gamma = 1.5°$. Looking at MPC data on the inclinations of the known objects, we found that the mean inclination of objects in the classical belt is 6.3° and that in the gap is 8.7°. Therefore the probability of finding an object at 6.3° relative to that at 8.7° is, $P(6.3°)/P(8.7°) = 1.385$. So to correct for this bias we need to multiply the gap population by 1.385.

So the overall bias from these two observational effects requires decrease by a factor of 0.862 in the value for the gap population used. This results in a decrease from the 7 objects quoted for the 40–41 AU region to 6.0 or about 3.2%, a decrease from 23 to 19.8 objects for the 42–42 AU region or about

10.7% and a decrease from 91 to 78.5 objects for the 42–43 AU region or about 42.4% of the densest part of the classical belt.

These statistics confirm the picture that the most unstable part of the belt is that which is nearest to Neptune, where even a low eccentricity cannot prevent encounters from taking place. Stability increases as the heliocentric distance increases, becoming essentially stable at around 43 AU. If we assume that the orbits of objects in the classical part of the belt beyond 43 AU are stable, then this population essentially represents the population that formed out of the primordial disk. So we take it that the population that formed out of the primordial disk with $40 < a < 43$ AU should have initially been similar to this population. Hence, we conclude that about 96.8% of the objects originally with $40 \leq a < 41$ AU have been lost, about 89.3% from the $41 \leq a < 42$ AU region and about 57.6% of the original population with $42 \leq a < 43$ AU. We have already argued that the reason for the loss of objects from the region $40 \leq a < 43$ AU is the gradual build up of eccentricity through planetary perturbations, which leads inevitably to a close encounter with Neptune. However, though the region concerned is sparsely populated, it is not empty; some objects have survived. A possible explanation for this is that the lifetimes of some of the objects in the region, while finite, are still greater than the age of the Solar System, and this is the main issue that we address in this paper.

We first investigated the lifetimes of hypothetical objects initially occupying a belt in the region from the location of the 3:2 mean motion resonance out to a semi-major axis of 43 AU. We assume that the initial population density and geometry of this region is similar to that found in the remainder (stable part) of the belt. This is described in more detail in Section 3.1. We also followed the orbital evolution of each of the hypothetical initial disk members to find out how they interacted with Neptune and the other planets and determine whether they escaped the system, became scattered disk members or fell into the inner Solar System.

Finally, there are actual objects in the 'gap', with known orbital elements, some well determined and others more poorly. Figure 3 is a plot of eccentricity against semi-major axis which shows the initial distribution of the real objects. It can be seen that most of the bodies have semi-major axes in the range $42 \leq a < 43$ AU. Specifically, there are only three real objects initially between 40 and 41 AU, 14 between 41 and 42 AU, and 49 between 42 and 43 AU. To take account of the possible inaccuracies in the published elements, we generated 405 clones with elements close to the published values. We integrated the equations of motion of the real objects, together with their clones, in order to determine their lifetimes and to compare their evolution with that of the hypothetical belt.

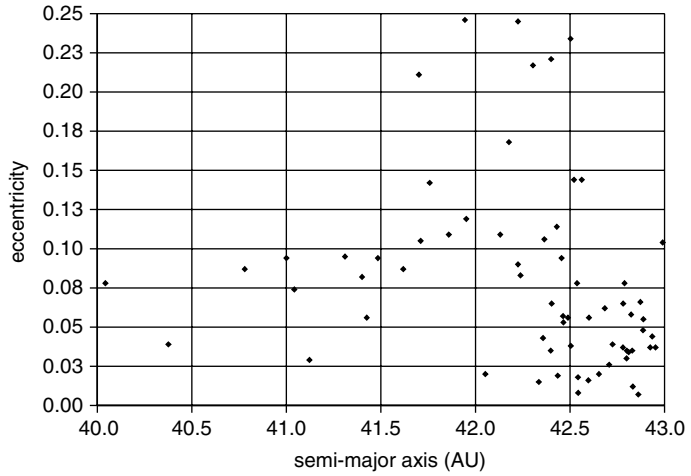

Figure 3. A plot of eccentricity against semi-major axis for observed Edgeworth–Kuiper Belt objects. This is a subset of the data used in Figure 1 concentrating on the semi-major axis range of interest, namely 40–43 AU.

3. The Evolution of the Hypothetical Inner Classical Belt

3.1. Numerical model

In this section we investigate the evolution of a hypothetical belt of objects initially having semi-major axes between that of Pluto's orbit and 43 AU, though for practical convenience we took the inner limit to be 40 AU. Our intention was to investigate this process within a Solar System with planets at the locations we find them today with gravity as the only force acting. That is, such forces which are not due to the gravitation of point like objects, are excluded. The problem here then is to ascertain what the likely distribution of orbits in this area is. The consensus of opinion is that the Edgeworth–Kuiper Belt reached its current configuration via the following sequence of processes. First that the proto-planetary disk is truncated at a certain heliocentric distance by one of several suggested mechanisms (see, for examples, Hollenbach and Adams, 2004; Melita et al., 2005; Kobayashi et al., 2005). Secondly, the outward migration of Neptune (see Malhotra, 1993, 1995; Fernandez and Ip, 1984) caused the formation of the resonant populations (again see Malhotra, 1993, 1995), the so called 'hot' population, that is those objects with high inclinations and eccentricities (see Gomes, 2003; Morbidelli and Levison, 2003), the scattered disk (see Duncan and Levison, 1997; Luu et al., 1997) and the 'cold' population (see Levison and Morbidelli, 2003).

As the portion of the belt we are concerned with is the cold classical part of the belt, we will use the results of the model of Levison and Morbidelli (2003) which involves the 2:1 mean motion resonance depositing objects in the

40–48 AU region as it migrates outward, resulting in a population of objects with eccentricities up to about 0.2. Hence, we restricted the eccentricity of the hypothetical objects in the initial belt to be less than 0.2, thus also ensuring that their initial perihelion distance is greater than 30 AU and that the objects are not immediately on Neptune crossing orbits. These authors also set the truncation of the proto-planetary disk at 30 AU (as in Gomes et al., 2004), this then means that all bodies currently in the Edgeworth–Kuiper belt formed within this 30 AU radius. It was shown by Malhotra (1995) that the 2:1 mean motion resonance does not excite inclinations thus we assumed that the inclinations in the initial classical belt in this region mirrors the geometry of the initial disk formed from the Solar Nebula. Papaloizou and Terquem (1999) showed that the standard accretion disk would have a height to radius ratio of about 1:7, which translates to an inclination limit of just under 10°. It was found also by Malhotra (1995) that there is a slightly enhanced concentration of objects around the weaker Neptune mean motion resonances in this region, for example the 5:3 resonance at 42.3 AU. We chose, however, to neglect these small density enhancements and began with a uniform semi-major axis distribution. There were no obvious reasons for restricting the remaining orbital elements, namely argument of perihelion, longitude of ascending node and mean anomaly, and so we assumed that they can take all values in the range 0° to 360°.

Integration for the age of the Solar System, even when using the most efficient methods, is computationally expensive, so the number of hypothetical objects to be investigated needed to be restricted. The number of objects currently in the stable part of the belt between 43 and 48 AU is slightly over 100 objects per 1 AU bin. Hence we generated 300 hypothetical objects to represent the initial population for the $40 \leq a < 43$ AU range. The values of all six orbital elements for each object were randomly selected from a uniform distribution with the following limits: $40 \leq a < 43$ AU, $0 \leq e < 0.2, 0° \leq I < 10°, 0° \leq \omega, \Omega, M < 360°$. The equations of motion for each hypothetical body were numerically integrated using Mercury 6 (Chambers, 1999). This is a hybrid symplectic integrator that changes from the symplectic integration to a Burlish–Stoer step by step integrator for close encounters, the change-over point used was 3 Hill radii from the centres of each planet. In the context of the Solar System, the Hill radius defines the approximate sphere of gravitational influence of a planet in the face of the gravitational perturbations from the Sun and is defined mathematically by

$$r_H = a\left(\frac{m_p}{3M_\odot}\right)^{1/3},$$

where m_p is the mass of the planet, a is its semi-major axis and $M_\odot$ is the mass of the Sun. Gravitational perturbations from the planets Jupiter, Saturn,

Uranus and Neptune were included in the equations of motion. Each object was integrated for up to 5×10^9 years, though to save on computation, the integration was terminated if the heliocentric distance of the object exceeded 300 AU or the eccentricity exceeded 1, since we then assumed that these objects were permanently lost from the Edgeworth–Kuiper Belt.

3.2. Results

The results of the calculations are represented by the position and velocity of each hypothetical object at each epoch, with a time interval of 10,000 years. From this a table of orbital elements for each object at each time interval can be produced. However, viewing the tables alone, or indeed showing in diagrammatic form the evolution of each object is not very instructive in illustrating the overall lack of stability in the region. From the calculated position of the object, we can determine whether the object was lost from the system, defined to be when its heliocentric distance exceeds 300 AU, and the epoch at which this occurs. From these data we determined the number lost up to any given epoch, and this is shown in Figure 4.

Figure 4 shows the number of objects surviving in the Solar System at a given time. From the orbital data, we can determine whether or not the semi-major axis of the orbit is still within the interval $40 \leq a < 43$ AU. Figure 5 is similar to Figure 4, except that it shows the number surviving with semi-major axes between 40 and 43 AU and shows how the gap population number dropped with time. We note that the general characteristics of both

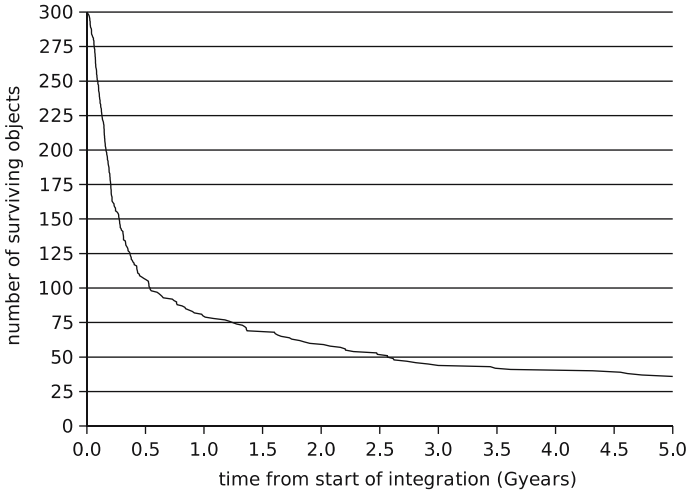

Figure 4. A plot showing the number of hypothetical objects still present within the Solar System after the indicated time.

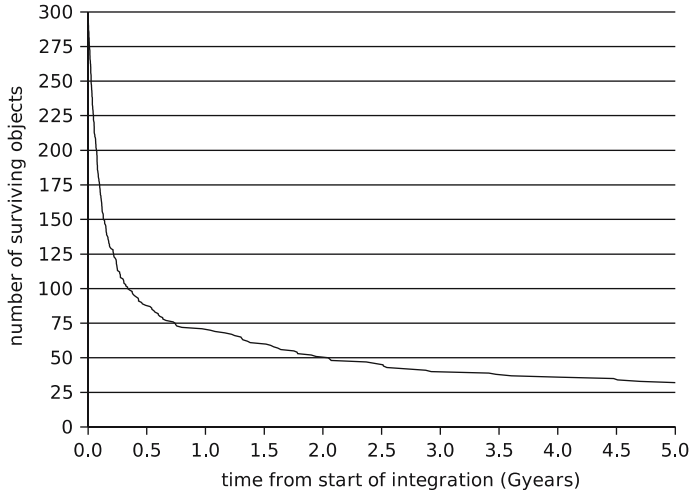

Figure 5. A plot showing the number of hypothetical objects that have remained within the region with $40 \leq a < 43$ AU up to the indicated time.

plots are very similar and that, as must obviously be the case, the number surviving between 40 and 43 AU is less than the number surviving in the Solar System.

If we consider the loss from the gap as illustrated in Figure 5, we see that after 5×10^9 years the population between 40 and 43 AU had dropped from the starting value of 300 to only 32. Looking at the three sub-intervals individually, the populations with $40 \leq a < 41$ AU has dropped to zero, while in the $41 \leq a < 42$ AU region only 4.5% of the initial population has survived, and in the $42 \leq a < 43$ AU region the figure is 26.5%. The relative values observed in the current population described earlier were 4.4%, 14.5% and 57.5% respectively. Hence we conclude that significantly more Edgeworth–Kuiper objects are found with $40 \leq a < 43$ AU than our simulation would suggest. There are two possible explanations for this. Either the objects that have actually survived are trapped in small islands of stability or they have been fed into the region of interest during the lifetime of the Solar System from some other region. In order to test the first hypothesis, we integrated the equations of motion of the real objects together with clones. This will be described later in Section 4.

Before doing that, it is instructive to follow the evolution of the hypothetical objects to determine how they are lost and what is responsible. In Figure 6 we show as Figure 6(a) the change in semi-major axis with time, Figure 6(b) shows the change in perihelion distance with time, Figure 6(c) shows the change in inclination with time, while Figure 6(d) is a plot of eccentricity against semi-major axis, each point representing the value at a given time. The solid curves in Figure 6(d) represent the locations where the

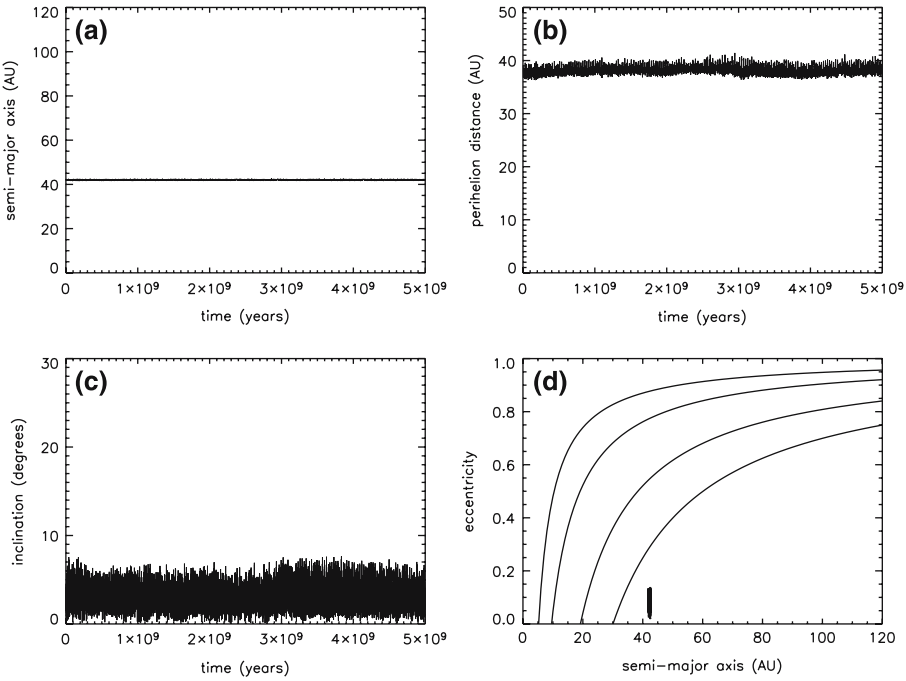

Figure 6. The first three sub-figures show the evolution with time of the three orbital elements a, q and I. The fourth sub-figure is a plot of eccentricity against semi-major axis, with each point representing the location of the hypothetical object after a time interval of 10^6 years. The solid curves in this sub-figure indicate where the perihelion of the orbit of the object is equal to the semi-major axis of Jupiter, Saturn, Uranus, and Neptune respectively.

object becomes a Neptune crosser, a Uranus crosser, a Saturn crosser and a Jupiter crosser, i.e. each line indicates where the perihelion distance of the object is equal to the semi-major axis of the planet. In principle we could plot the changes in all the orbital element against time, but these are not very instructive. In Figure 6(b) we see that, as predicted, perturbations cause changes in perihelion distance. However these remain bound throughout the time interval with the perihelion distance remaining between about 36 and 41 AU. In Figure 6(d) we see that there is very little change in the semi-major axis but that the eccentricity oscillates between 0 and 0.15. This is, in fact, a rather uninteresting plot, but it shows how the evolution of an object that survives for the full integration interval can be rather uneventful. There are 25 such figures, representing the 25 objects that survived the whole integration with no major change in their orbits.

There were also nine objects which moved from their initial unstable orbits onto stable orbits still within the gap region, and remained there for the rest of the simulation. These objects have found orbits which lie on small islands of stability within the otherwise unstable region. Figure 7 shows an

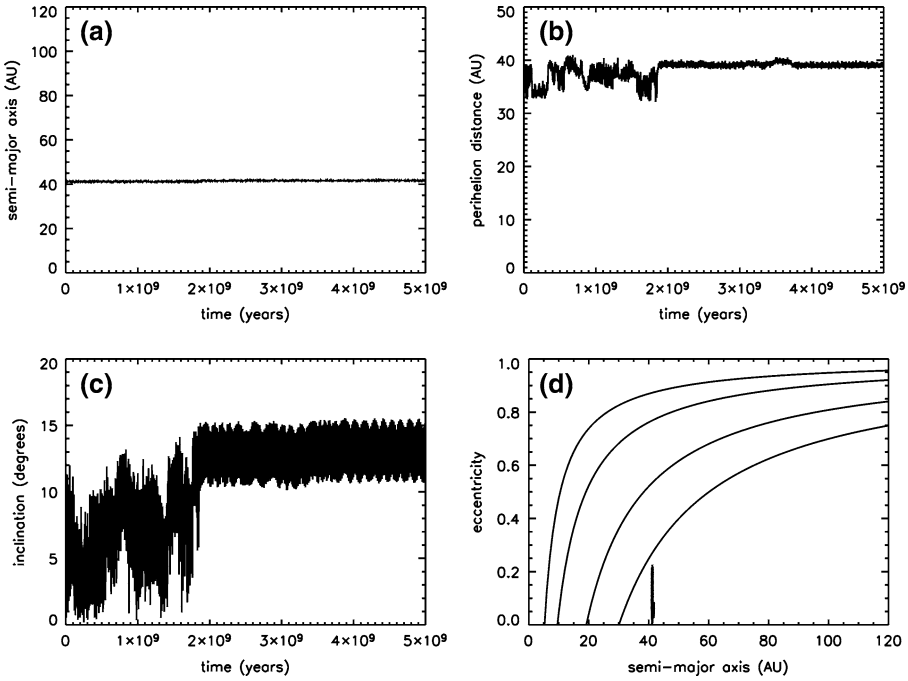

Figure 7. This plot shows the evolution of a hypothetical object which is not lost from the gap, but moves onto a stable orbit within the gap after 2×10^9 years.

example of this. The plots are similar to Figure 6, but here we can see that while the semi-major axis remains close to its initial value, the perihelion distance and inclination vary significantly for the first 2×10^9 years before the object settles into an orbit with inclination osculating around 13° and perihelion distance steady at about 39 AU (corresponding to an eccentricity of 0.06).

Figure 8 is again similar to Figure 6, except that this is for an object that was lost after about 1.84×10^8 years. Plots (a), (b) and (c) only show the interesting evolution at the end of the object's time in the gap, from 1.5×10^8 years after the start of the simulation. Plot (d) shows the whole evolution with the interval between data points being 10^4 years, this is true for plot (d) in all of Figures 8–11. In Figure 6 the interval is increased to 10^6 years and in Figures 7 and 12 to 10^5 years. The reason for this is simply one of practical convenience; because these plots show the evolution for the whole 5×10^9 years it was necessary to reduce the number of plotted points in order to make the actual image files manageable. We see from Figure 8 that this very much represents the situation that we described in the introduction, namely perturbations causing changes in eccentricity and perihelion distance that eventually lead to a close encounter with Neptune. At this point, the object was lost very rapidly, there being no point in Figure 8(d) showing any situation

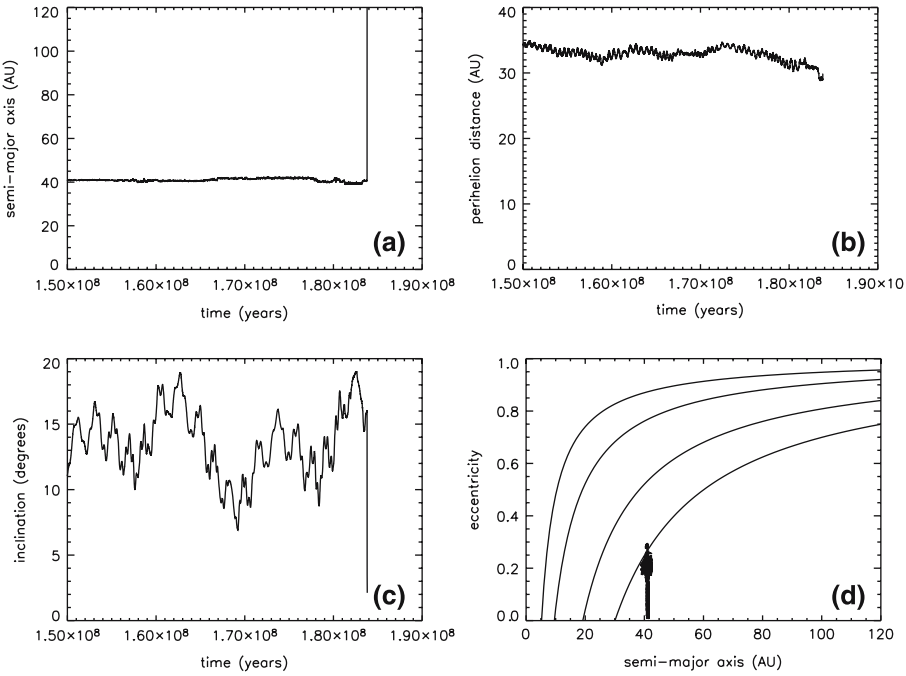

Figure 8. This plot shows the last 3.4×10^7 years of the evolution of a hypothetical object which is lost from the 40–43 AU gap after a close encounter with Neptune after 1.83×10^8 years.

between becoming a Neptune crosser and being lost from the system. This, however, is an unusual case, only this one object was ejected so rapidly after encountering Neptune.

Figure 9 is again similar, but shows an object where ejection from the system took longer. Again we show only the last part of the object's evolution in plots (a), (b) and (c) in order for the more interesting details to be clearly visible, in this case the plots show the evolution after 5×10^8 years. We see the increase in eccentricity leads to close encounters with Neptune after around 5.4×10^8 years. However the object is not lost for a further 6×10^6 years, remaining, as we see from Figure 9(b) with perihelion close to the orbit of Neptune for this interval, but with both a and e increasing (as seen from Figure 9(d)). In the final stages before being lost, this object has an orbit very similar to many in the scattered disk, with semi-major axis of over 100 AU and eccentricity in the range 0.6–0.8. There were 50 objects with behaviour similar to this.

Figures 10 and 11 are again similar to the previous four figures but show that some objects have a more complex evolution. The evolution of the object in Figure 10 is shown in plots (a), (b) and (c) from 7.5×10^7 years after the start of the integration. The semi-major axis of this object remains fairly

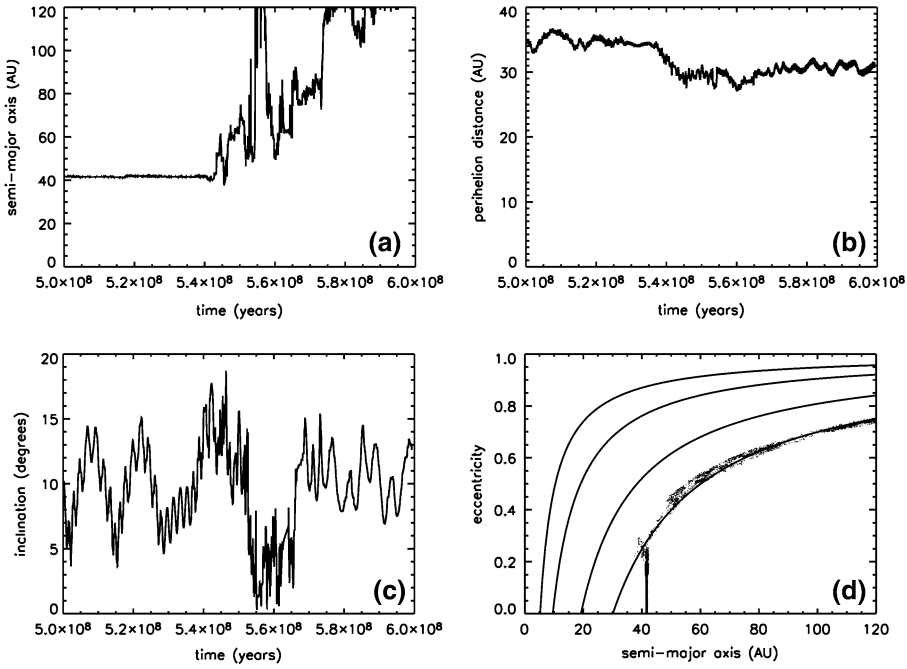

Figure 9. Plot showing the evolution of a hypothetical object which is lost from the Solar System after 6×10^8 years. In the first three sub-figures only the evolution for the last 10^8 years of evolution is shown.

constant until a close approach with Neptune causes a perihelion decrease and there is a short time interval where perihelion is close to the orbit of Uranus. As can be seen from Figure 10(b), this situation does not persist and the object becomes a Saturn crosser before being lost. The whole evolutionary phase for this object is only 9.5×10^7 years and the stage where perihelion is close to Saturn lasts for only about 10^6 years. Because of this short interval, it is unlikely that we could ever observe an actual object behaving in this fashion, and to date none such have been observed. 113 of our hypothetical objects were lost after close encounters with Saturn; in fact this was the most common method for ejection.

Figure 11 shows the evolution of an object that is lost from the system having survived for just under 10^9 years and the plotted evolution in plots (a), (b) and (c) starts at 9.6×10^8 years. Again the initial evolution is as in other cases where it has an interval with close Neptunian encounters. Like the object shown in Figure 10, it then spends a short time close to Uranus and a further short time close to Saturn before eventually being lost when the eccentricity increases past the point where perihelion is inside the orbit of Jupiter. This object reaches values of a and e that are consistent with values for long period comets. As can be seen in Figure 11(c), the inclination at this

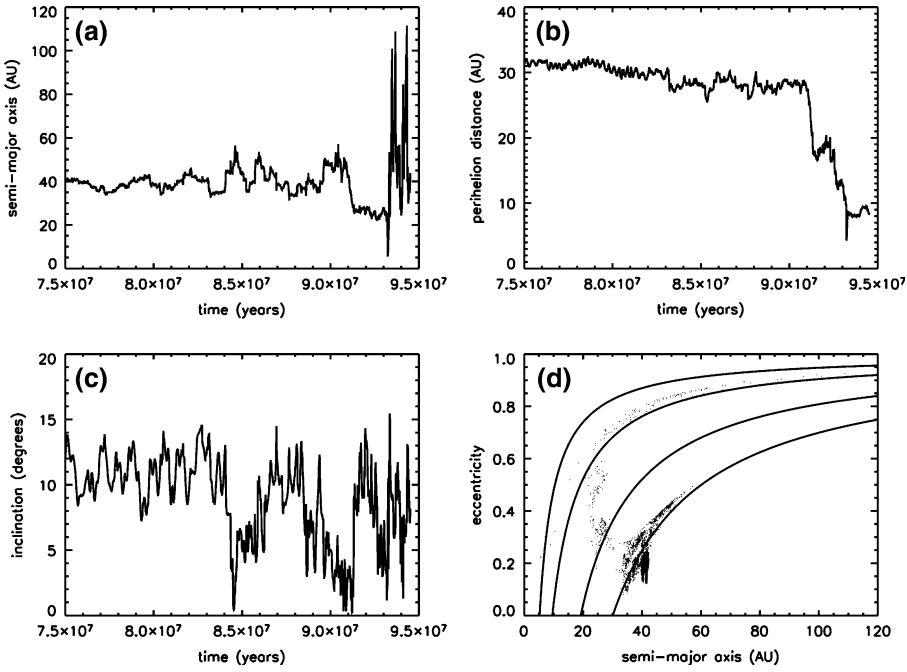

Figure 10. Plots showing the last 2×10^7 years of evolution of a hypothetical object which is lost from the Solar System after multiple encounters with Neptune, Uranus and finally Saturn beginning at about 8×10^7 years after the beginning of the simulation and resulting in the object being lost at about 9.5×10^7 years.

stage has also increased to more than 45°. This, of course, is not a mechanism for generating most long period comets, but it does suggest that a few could have originated from the inner Edgeworth–Kuiper Belt. The number of objects which were finally ejected by Jupiter is 69. This figure also illustrates how the stage of an object's evolution after it has moved out of the gap can be extremely small compared to its gap lifetime. The vast majority of this object's evolution is spent in the gap making oscillations in e, visible as the dense vertical bands in Figure 11(d). Similar features can be seen in all plots (d) in Figures 6–12.

In three cases the hypothetical bodies moved into a long lived orbit beyond Neptune in which they did not encounter Neptune again for the remainder of the simulation (cf. Malhotra et al., 2000). Figure 12 shows an example of this. As in the other figures, perturbations cause changes in the perihelion distance which results in the object crossing Neptune's orbit. This first occurs after about 2.5×10^8 years. Subsequently, the semi-major axis of the orbit is increased and the object moves into an orbit which is not Neptune crossing. Eventually the object settles into an apparently stable orbit with semi-major axis of about 80 AU and eccentricity just below 0.6.

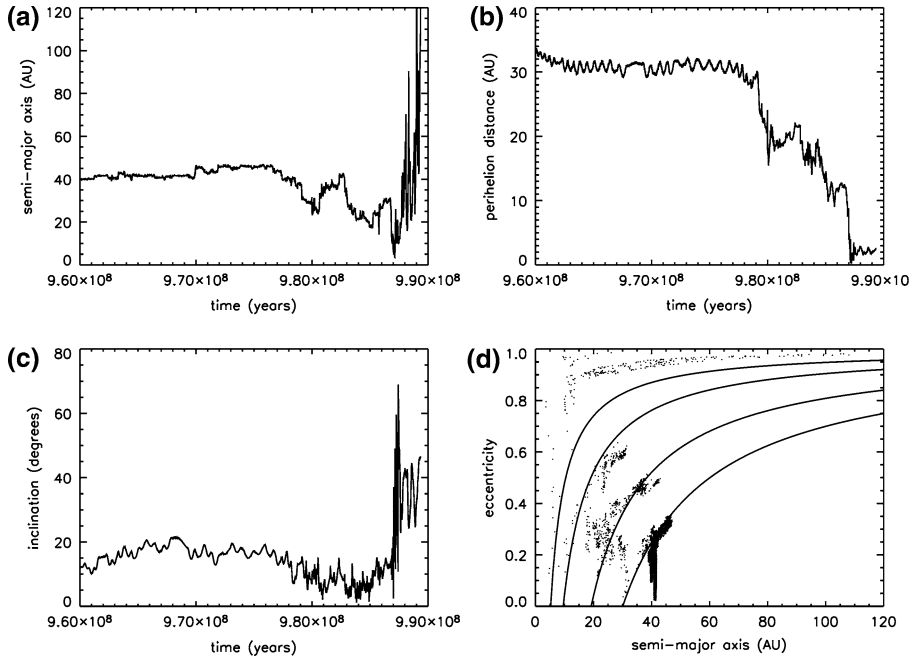

Figure 11. Plots showing the final 3×10^7 years of the evolution of a hypothetical object which is lost from the Solar System after multiple encounters with all the giant planets and finally being lost due to Jupiter. The object does not cross the orbit of Neptune until about 9.63×10^8 years and is lost from the Solar System at about 9.9×10^8 years.

None of the evolution calculations show any objects leaving the gap and then subsequently returning to a long lived orbit back inside the gap. That is to say, once an object's semi-major axis leaves the interval 40–43 AU, it never returns to it.

4. The Evolution of the Real objects and their Clones

4.1. Model

As mentioned above, the number of hypothetical objects initially located with a semi-major axis in the range $40 \leq a < 43$ AU that survived in our simulation was considerably less than the relative numbers observed in the real belt. This could be because the real objects were, by chance, located on islands of stability, or because they are recent insertions into the gap. In this section we tested the first of these possibilities by integrating the equations of motion of the real objects for the same time interval, 5×10^9 years. The orbital elements were taken from the Minor Planets Center website (http://cfa-www.harvard.edu/iau/mpc.html). To ensure that objects with well

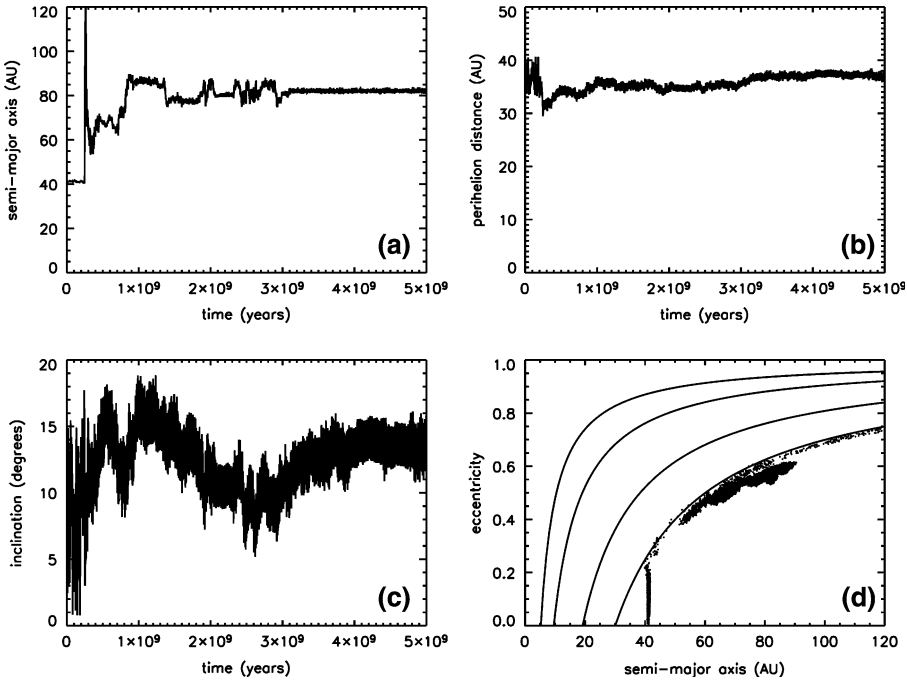

Figure 12. Plots showing the evolution of a hypothetical object which is not lost from the Solar System after the whole integration, but leaves the gap quickly. The object comes close to the orbit of Neptune at about 3×10^8 years, but its orbit then moves outwards and eventually settles at an orbit with a just above 80 AU, where it remains until the end of the simulation.

defined orbits were used, only those objects which have been observed at two or more oppositions were included. This means that the number of objects considered here is less than the number shown in the histogram in Figure 2, which shows all of the objects which have been discovered. Each set of opposition observations improves the quality of the orbital elements and it is generally found that for objects observed at more than three oppositions the orbits are very secure. Thus for such objects only the body with its published elements was investigated. There are 21 such objects. For those observed less frequently, nine clones were also produced for each object, with their orbital elements within a range of plus or minus half the magnitude of the smallest figure reported. Thus for example, if the published eccentricity is 0.67, clones were generated with eccentricities in the range 0.665–0.675. Only errors in eccentricity, semi-major axis and inclination were considered, with three clones created in the error range for each of these three elements. 12 Edgeworth–Kuiper objects have been observed at two oppositions and 33 observed at three oppositions, making a total of 45 objects that required clones. Thus in this section we integrated in total $45 \times 9 = 405$ clones and 66 real objects, making a total of 471 objects.

4.2. Results

The dynamical behaviour of the real objects and their clones is similar to the behaviour of our hypothetical ones in the sense that no dynamical behaviour was identified that was substantially different from one of the sets illustrated in Figures 6–11. What is dramatically different is the fraction of objects that behave in the different ways. Consider first the 21 objects that have been observed at more than three oppositions and thus have a very well determined orbit. Out of these, 13 (62%) have remained in orbits close to their initial orbits throughout the integration interval of 5×10^9 years, in contrast to the large loss of hypothetical objects, where only 11% survived for the same time interval.

Looking at the 45 real objects that have been observed at three oppositions or fewer, a similar picture emerges, though analysis is more complex as each object now also has nine clones to be considered. Of these 45 objects, in 33 cases, the object and all nine of its clones survived for the whole integration. These 33 real objects, or 73% of the total, are thus moving in very stable orbits. At the other end of the scale, three objects and every clone of each of them were lost, indicating that at least 7% of the real group is unstable. Of the remaining nine objects, one survived while all nine of its clones were lost. This object should be regarded as being unstable. Three objects, together with some, but not all of their clones survived, and five real objects were lost while some of the clones of each of them survived. Even if we regard every object in this last group of nine as being lost, the total number of real objects that survived for 5×10^9 years is 46 out of 66 (70%), compared to 11% for the hypothetical objects. The real objects appear to be on much more stable orbits than the hypothetical ones and it is interesting to discuss possible reasons for this.

It should be emphasised that the real objects and the hypothetical ones are not dynamically equivalent sets, and there are two differences that could be significant. The hypothetical objects had inclinations that were distributed uniformly in the range $0^\circ \leq I < 10^\circ$ and the semi-major axes were uniformly distributed in the range $40 \leq a < 43$ AU, while for the real objects, there is no such restriction. In fact the inclinations of the real objects near the inner edge of the gap are significantly higher as can be seen in Figure 13. A higher value of inclination implies that the object spends less time close to the ecliptic which in effect reduces the probability of experiencing a close encounter with Neptune (which orbits close to the ecliptic plane), and thus of being perturbed out of the system.

A second difference concerns the distribution of the semi-major axes. As we have seen in Figures 3 and 13, the real objects are predominantly situated in orbits with semi-major axes in the range 42–43 AU; specifically there are only three real objects with semi-major axes initially between 40 and 41 AU,

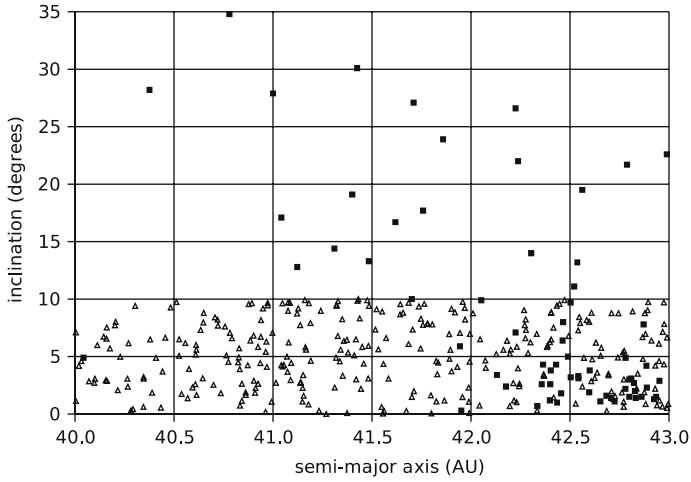

Figure 13. A plot of initial inclination against semi-major axis for all the real and hypothetical objects. Real objects are shown as filled squares and hypothetical objects as empty triangles. The higher inclinations of the real objects are clearly visible.

14 between 41 and 42 AU, and 49 between 42 and 43 AU, while for the hypothetical objects, the semi-major axes were uniformly distributed between 40 and 43 AU. We have already stated that the range 42–43 AU is the most stable range of the three considered, but even here only 26.5% of the hypothetical objects survived, a factor of three below the survival rate for the real objects.

Inspecting the data in more detail, there are some curious results. All but one of the set of real objects and clones between 40 and 41 AU have remained in very stable orbits throughout the integration interval and the one exception is a clone. Conversely, there are several objects beyond 42 AU which do not survive for the whole integration time (see Figure 14). This figure also shows that the clones are, in many cases, ejected at a different time to the corresponding real object, suggesting that the stability of orbits in the neighbourhood of the real objects' orbits is very variable, with only small deviations changing the orbits from stability to instability. This is to be expected in a chaotic environment, where small islands of stability can exist within a sea of instability.

5. Conclusions and Discussion

In this paper, we have investigated the survival of a set of 300 hypothetical objects with initial semi-major axes in the range $40 \leq a < 43$ AU and other orbital elements chosen to simulate the conditions after planetary migration.

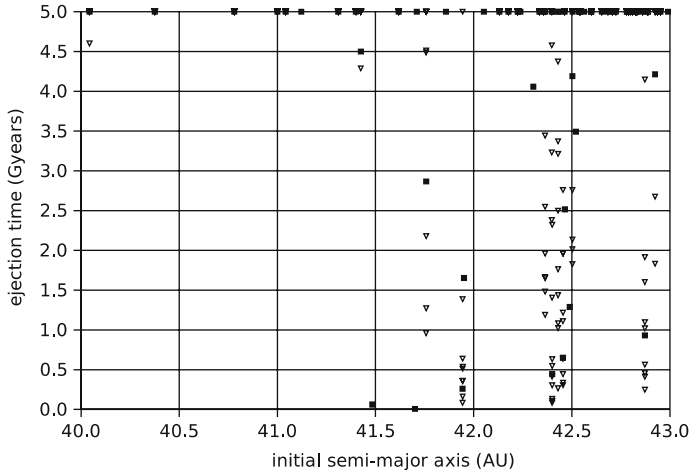

Figure 14. A plot of time of ejection from the gap against initial semi-major axis for all the real and clone objects. Real objects are shown as filled squares and clone objects as empty triangles.

After integrating for 5×10^9 years, we find that the populations in the range $40 \leq a < 41$ AU has dropped to zero, while in the range $41 \leq a < 42$ AU only 4.5% of the initial population has survived and in the $42 \leq a < 43$ AU region the figure is 26.5%. In the real population we observe about 185 objects per 1 AU gap in the region $43 \leq a < 45$ AU, whilst in the region $40 \leq a < 41$ AU there are seven objects, which including a debiasing factor represents about 3.2% of that observed in the 43–45 AU region. The population with $41 \leq a < 42$ AU numbers 23 objects or about 10.7% of population of the densest region taking account of biases, while the population with $42 \leq a < 43$ AU is about 91 objects or, taking account of biases, 42.4% of the densest region. We also find that the real objects are in general in stable orbits that can survive for the age of the Solar System.

There are two possibilities to explain this discrepancy in numbers:

1. Objects in the observed population are on small islands of stability in a generally unstable region, allowing more than expected to survive. Although in general the gap region is unstable, the complexity of the forces and the chaotic nature of the system as a whole can result in small regions of relative stability on long timescales. The integration of hypothetical objects does show nine objects which move from their initial orbits onto long lived orbits inside the gap, showing that such islands of stability do exist. A further 25 objects remain in their initial orbits, but the overall number which survive in the gap is not enough to match the real population. Therefore it may be that evolution under the

influence of gravitational perturbations from the planets as we see them now is not the primary cause for this. Perhaps then the real objects we see in these stable orbits were placed there by some process associated with migration.

2. The initial population between 40 and 43 AU was much higher than we have assumed (which would have to be higher than the population of objects captured in the 3:2 mean motion resonance). Our hypothetical simulation started with an even distribution in semi-major axis for the gap region and we assumed that the population density in the classical belt would be similar. It is likely that this was not the case in the real Solar System. In fact Malhotra's (1995) work indicates that the number of objects after migration is greater outside 43 AU. However, this is contrary to what we require and would make the discrepancy in numbers even worse.

Both of the above possibilities are reasonable hypotheses, but of course it is possible that a more outlandish explanation can be provided. For example that objects have recently been captured in the region between 40 and 42 AU. One mechanism for maintaining the gap population may be collisions within the classical belt. Another possible mechanism which could be moving objects into the gap is the passage of large, as yet undiscovered TNOs which move through the dense classical Edgeworth–Kuiper Belt. This possibility is highlighted by the recent discovery of 2003 UB313. Although 2003 UB313 currently crosses the ecliptic at about 89 AU, well away from the classical belt, it is conceivable that similar objects which do move through the classical belt could still remain undiscovered. In fact, recent movement into the gap must have happened for some of the real objects we have investigated as their stable lifetimes are very short and thus are not on islands of stability, however the mechanisms we suggest are purely speculative and need to be simulated to be checked.

We have also investigated the process by which objects are lost. We expected a simple slow evolution until a close encounter with Neptune ejected the object, but the results proved to be more interesting than this. In many cases the object became a Uranus or Saturn crosser and in a few cases even a Jupiter crosser. In the latter stages of their life some of the objects had orbits resembling those of objects in the scattered disk, though the lifetime in such orbits was short.

In summary, the results suggest that there is more to consider than simply gravitational perturbations from the known planets, and that the possible processes given above deserve further study. Also we have shown that the evolution of Edgeworth–Kuiper Belt objects can be complex if they are perturbed into Neptune crossing orbits.

Acknowledgements

DCJ would like to acknowledge PPARC for the award of a studentship which allowed this work to be carried out, and the University of London's Valerie Myerscough Prize which helped finance his attendance at ACM 2005. Also the authors thank Rodney Gomes for constructive comments which led to improvements in the paper.

References

Binzel, R. P.: 1989, in R. P. Binzel, T. Gehrels, M. S. Matthews, (eds.), *Asteroids II*, University of Arizona Press, Tucson, pp. 3–18.
Chambers, J. E.: 1999, *Mon. Not. R. Astron. Soc.* **304**, 793–799.
Collander-Brown, S. J., Fitzsimmons, A., Fletcher, E., Irwin, M. J., and Williams, I. P.: 2001, *Mon. Not. R. Astron. Soc.* **325**, 972–978.
Collander-Brown, S. J., Melita, M. D., Williams, I. P., and Fitzsimmons, A.: 2003, *Icarus* **162**, 22–26.
Duncan, M. J. and Levison, H. F.: 1997, *Science* **276**, 1670–1672.
Duncan, M. J., Levison, H. F., and Budd, S. M.: 1995, *Astron. J.* **110**, 3073–3081.
Duncan, M., Quinn, T., and Tremaine, S.: 1988, *Astrophys. J. Lett.* **328**, L69–L73.
Edgeworth, K. E.: 1943, *J. Brit. Astron. Assoc.* **53**, 181–188.
Fernandez, J. A., Gallardo, T., and Brunnini, A.: 2003, *EM&P* **92**, 43–48.
Fernandez, J. A. and Ip, W.-H.: 1984, *Icarus* **58**, 109–120.
Gladman, B., Holman, M., Grav, T., Kavelaars, J. J., Nicholson, P. D., Aksnes, K., and Petit, M. J.: 2001, *Icarus* **157**, 269–279.
Gomes, R. S.: 2003, *Icarus* **161**, 404–418.
Gomes, R. S., Morbidelli, A., and Levison, H. F.: 2004, *Icarus* **170**, 492–507.
Hollenbach, D. and Adams, F. C.: 2004, in L. Caroff, D. Backman, (eds.), *Debris Disks and the Formation of Planets*, ASP, San Francisco, pp. 168–183.
Jewitt, D. C. and Luu, J. X.: 1993, *Nature* **362**, 730–732.
Kobayashi, H., Ida, S., and Tanaka, H.: 2005, *Icarus* **177**, 146–255.
Kowal, C.: 1989, *Icarus* **77**, 118–123.
Kuiper, G. P.: 1951, in J. A. Hynek, (ed.), *Astrophysics, A Topical Symposium*, McGraw-Hill, New York, pp. 357–424.
Levison, H. F. and Morbidelli, A.: 2003, *Nature* **426**, 419–421.
Luu, X. J., Marsden, B. G., Jewitt, D. C., Trujillo, C. A., Hengrother, C. W., Chen, J., and Offutt, W. B.: 1997, *Nature* **387**, 573–575.
Malhotra, R.: 1993, *Nature* **365**, 819–821.
Malhotra, R.: 1995, *Astron. J.* **110**, 420–429.
Malhotra, R., Duncan, M. J., and Levison, H.: 2000, in V. Mannings, A. P. Boss, S. S. Russell, (eds.), *Protostars and Planets IV*, University of Arizona Press, Tucson, pp. 1231–1245.
Maran, M. D. and Williams, I. P.: 2000, *Mon. Not. R. Astron. Soc.* **318**, 482–492.
Melita, M. D., Williams, I. P., Collander-Brown, S., and Fitzsimmons, A.: 2004, *Icarus* **171**, 516–524.
Melita, M. D., Larwood, J. D., and Williams, I. P.: 2005, *Icarus* **173**, 559–573.
Morbidelli, A. and Levison, H. F.: 2003, *Nature* **422**, 30–31.
Papaloizou, J. C. B. and Terquem, C.: 1999, *Astroph. J.* **521**, 823–838.

Quinn, T., Tremaine, S., and Duncan, M.: 1990, *Astroph. J.* **355**, 667–679.
Stagg, C. R. and Bailey, M. E.: 1989, *Mon. Not. R. Astron. Soc.* **241**, 507–541.
Trujillo, C. A., Jewitt, D. C., and Luu, J. X.: 2001, *Astron. J.* **122**, 457–473.
Tsiganis, K., Gomes, R., Morbidelli, A., and Levison, H. F.: 2005, *Nature* **435**, 459–461.
Williams, I. P., Fitzsimmons, A., O'Ceallaigh, D., and Marsden, B. G.: 1995, *Icarus* **116**, 180–185.